11th Australasian Fluid Mechanics Conference
University of Tasmania, Hobart, Australia
14-18 December 1992

ON THE HYDRODYNAMIC INSTABILITY OF THE WALL JET

M.D. ZHOU, J. ROTHSTEIN and I. WYGNANSKI

Department of Aerospace and Mechanical Engineering
University of Arizona, Tucson AZ 85721, USA

ABSTRACT

The spatial amplification of disturbances in a laminar wall jet was investigated theoretically and experimentally. Two closely coupled, unstable eigen modes were observed over a wide range of Reynolds numbers and frequencies and their influence on the amplitude and phase distributions is discussed.

INTRODUCTION

A simple idea equating a large coherent structure observed in a turbulent free-shear flow with the predominant instability to which such a flow is susceptible, enabled us to predict, alter and to a large extent control the behavior of many free shear flows (e.g. a turbulent mixing layer, a wake or a jet). The extension of these ideas to wall bounded flows is not straightforward because a small number of instabilities, generated concomitantly, may coexist and interact in a wall bounded flow. A turbulent boundary layer, for example, contains at least two clearly identifiable scales one affiliated with the wall region while the other with the outer flow. It is therefore quite possible that the tedious search for definitive coherent structures in a boundary layer (which is inviscidly stable in the mean), stems from the difficulty in identifying the dominant instability modes. The instability near the wall is probably dominated by viscosity while the instability in the outer flow might be inviscid as it is associated with the "wake region". We turned our attention to a turbulent wall jet embedded in a uniform stream, because in this case we can alter the strength and significance of the inviscid instability of the outer region. Furthermore, we started to consider the effects of streamwise curvature and pressure gradient because of their influence on the wall region in the hope of resolving the intricate interactions between the outer and the inner structures existing in a typical turbulent boundary layer.

However, the evolution of harmonic perturbations in a turbulent wall-jet posed some new difficulties not encountered in the free shear flows considered. To begin with, the complex interaction between the coherent motion and the "incoherent turbulence" did not have to be accounted for, in the initial stability calculations of the unbounded flows. Since these flows were dominated by an inviscid instability, the Rayleigh equation represented the lateral distribution of the leading coherent fluctuations very well (e.g. see the comparisons made by Weisbrot and Wygnanski 1988 for the case of a turbulent mixing layer). Consequently the question of a representative Reynolds number in a turbulent flow did not arise. Since the primary instabilities near the surface of the wall jet are affected by viscosity, the full Orr-Sommerfeld equations containing Re as a parameter had to be considered.

The concomitant interactions among a small number of linearly generated modes of instability makes the identification of a predominant mode extremely difficult. The non linear interactions between the coherent and incoherent fluctuations may provide a cascade mechanism through which the effects of viscosity are further enhanced. Some of these interactions were lumped together into an equivalent viscous term by introducing an eddy viscosity (Liu 1971; Tam & Chen 1979 and Marasli 1989) which led to a fictitious Re used in solving the Orr-Somerfeld equation. This choice introduced an indeterminacy not present in the inviscid calculations. It should be stressed that the choice of an eddy viscosity is arbitrary and it can not express realistically a physical mechanism existing in the flow.

A comparison between the measured and the calculated amplitude and phase distributions in a forced turbulent wall jet made by Katz et al. (1992) proved to be inferior to the agreement achieved in free shear flows (Weisbrot et al. 1988; Marasli et al. 1989). The possible reasons for this inferiority are many and they are too complicated to be positively identified without a comprehensive understanding of the instabilities encountered in the laminar wall jet. Surprisingly however, very little experimental information is available about the stability of this laminar flow.

The plane laminar wall-jet flowing over a flat surface in the absence of an external stream possesses two modes of temporal instability provided the Reynolds number is sufficiently large (Chun & Schwarz 1967; Tsuji et al. 1977 and Mele et al. 1986). The large scale (low frequency) disturbances are associated with the outer inflection point in the mean velocity profile while the small scale unstable disturbances evolve mostly near the surface. A limited number of spatial stability calculations done at Re=800 and 900 (Cohen et al. 1992) also predict the existence of two spatially amplified modes. Some power spectra measured near the surface and in the outer flow suggest that both the laminar and the turbulent wall jets contain two dominant scales (Cohen et al. 1992; Katz et al. 1992) in contrast to most free shear flows which are naturally (i.e. without external forcing) dominated by a single scale. Tsuji et al

(1977), who excited the laminar wall jet acoustically failed to confirm the existence of a second instability mode in their experiment, while Katz et al. did not manage to predict its possible existence in a turbulent wall jet at any of the Reynolds numbers which they considered.

The main purpose of the present investigation is to determine the range of parameters (both frequencies and Reynolds numbers) giving rise to spatially amplifying waves in a laminar wall jet and to confirm the calculations experimentally for both modes of instability. Based on these findings, the interaction between the modes can be quantitatively specified. The effects of streamwise curvature on the relative importance of each mode is also explored for the purpose of providing a better correlation between the coherent structures in the turbulent wall jet with the predominant instability modes.

ANALYSIS

The spatial evolution of a small amplitude, two dimensional wavy disturbance is described by assuming a perturbation stream function of the form:

$$\psi(y,t) = \phi(y)\, e^{[i(\alpha x-\beta t)]} \qquad (1)$$

where $\beta(x) \equiv [2\Pi\ f\ Y_{m/2}/U_m]$ represents a real frequency parameter and $\alpha(x) = [\alpha_r + i\alpha_i]$ represents a complex wave number. All the velocities in equation (1) are normalized by the maximum velocity in the wall jet U_m and all length scales are divided by the local half-width of the jet $Y_{m/2}$, thus:

$$x=\frac{X}{Y_{m/2}},\quad y=\frac{Y}{Y_{m/2}},\quad t=\frac{TU_m}{Y_{m/2}},\quad \psi=\frac{\Psi}{U_m Y_{m/2}}\ .$$

The eigenfunction $\phi(x,y)$ satisfies the Orr-Sommerfeld equation:

$$(U-c)(\phi''-\alpha^2\phi)-U''\phi+\left[\frac{i}{\alpha Re}\right][\phi^{iv}-2\alpha^2\phi+\alpha^4\phi]=0 \qquad (2)$$

subject to boundary conditions;

$$\phi_{y=0} = \phi_{y=\infty} = 0 \quad \text{and} \quad \left[\frac{\partial\phi}{\partial y}\right]_{y=0} = \left[\frac{\partial\phi}{\partial y}\right]_{y=\infty} = 0$$

Because equation (2) is solved locally for each $U(x,y)$, the eigen values α and β depend on x and on the Reynolds number $Re \equiv U_m Y_{m/2}/\nu$.

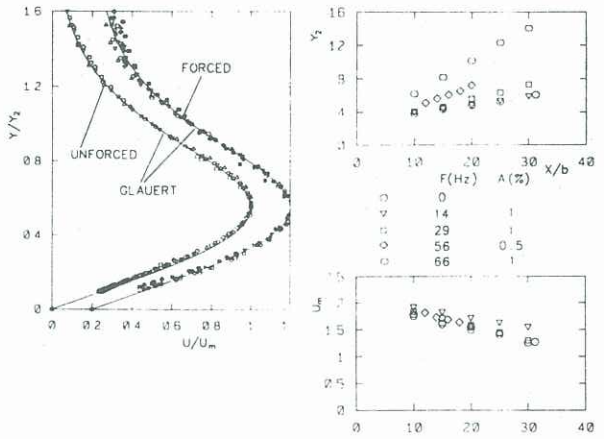

Fig.1 The mean velocity field.

The phase velocity of the disturbance $c = \beta/\alpha_r$. Gram-Schmidt orthonormalization procedure was used to solve equation (2) because the coefficient $(i/\alpha Re)$ multiplying the highest derivative in this equation in is very small. Since the normalized velocity profile (fig. 1) agreed fairly well with Glauert's (1956) analytical solution the latter was used as an input in the stability calculations.

One starts the solution process at a prescribed Re by guessing $\alpha(x)$ and improving on the guess until the boundary conditions are satisfied. The neutral stability curve and the curves of constant amplification-rate were calculated by prescribing α_i and Re while guessing α_r and β but a cross check was made by alternating between the prescribed and the guessed parameters. The results of these computations (fig. 2) indicate that the critical Re = 57 and corresponds to the dimensionless frequency (or Strouhal number) β = 0.565. This value of β corresponds to the occurrence of the maximum amplification rate at low Re (i.e. for 100 < Re < 200), and also to the stable region which exists between Re = 377 and Re = 456. The appearance of the stable region in the midst of an amplified zone is peculiar to the wall jet. It was calculated first by Chun and Schwarz (1967) but it extended between 370 < Re < 750. The discrepancy between the present results and the earlier computations may stem from small round-off errors in an interpolation subroutine when large increments in Re were used. For β > 0.58, the waves are amplified above the appropriate critical Re as well as for β < 0.56. Thus there is a very small range of frequencies and Reynolds numbers at which the waves might decay at Re which exceeds the initial critical value by a factor of 6. The highest frequency to which the wall jet is unstable is β = 1.65 and it occurs at Re ≅ 400.

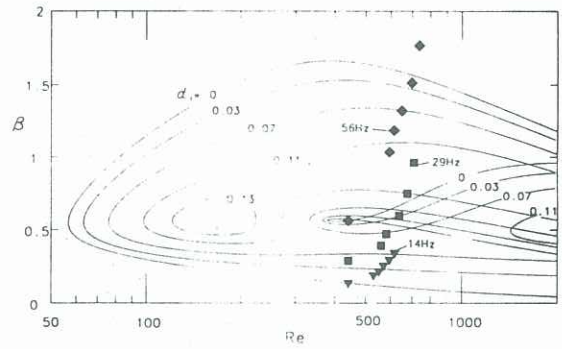

Fig.2 Contours of spatial amplification.

The wall jet is susceptible to two modes of instability which might be strongly coupled in the range of Re considered. At moderately high Re (Re > 500), the unstable large scale streamwise disturbances have their maximum amplitude near the outer inflection point. These disturbances are dominated by inertia and may be considered as being "inviscidly unstable". For example: the amplitude distribution computed for the lower branch of the neutral stability diagram (at Re = 890 & β =0.1 in fig.3) resembles the amplitude distribution computed for the sinuous mode of a plane half-jet. There is a slight distortion near the wall to accommodate the boundary condition requiring that the normal velocity perturbation will vanish there, such a requirement does not exist on the plane

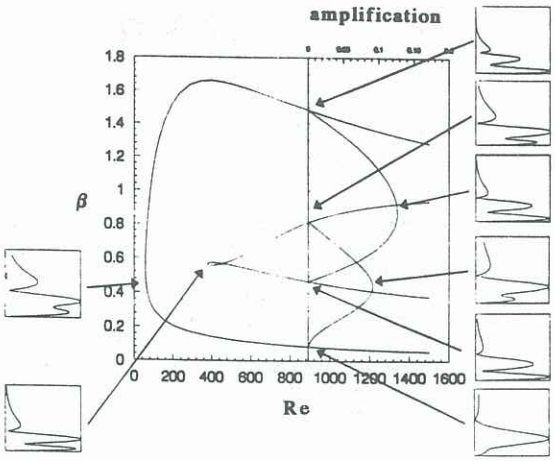

Fig.3 Neutral stability curve, amplification rates and amplitude distributions in the wall jet.

of symmetry of a jet or a wake. On the other hand, the small scale disturbances (β = 1.48 & Re = 890) near the upper branch of the neutral stability curve have their highest amplitude near the surface. The amplification rates (which are cross plotted on fig. 3 at Re = 890) indicate that both modes amplify when $0.45 < \beta < 0.8$. Growing disturbances of a prescribed frequency in this region, might have a different amplitude distribution across the wall jet depending on the mode of instability computed (fig. 3). At low super critical Re the importance of the viscous terms in the O-S equation is larger and they affect the shape of the computed eigen functions even at the lowest amplified frequencies. The two amplified modes are inseparable at $57 < Re < 377$.

The wave length associated with a prescribed frequency becomes discontinuous at Re =377 and it is double valued in the region at which both modes are amplified (fig. 4). This fact might enable one to identify experimentally the predominant mode of a prescribed frequency existing in the flow.

EXPERIMENTS

The experiments were carried out in a low turbulence wind tunnel as a part of a comprehensive study of wall jets in streaming flow. The flow originated from a two dimensional nozzle spanning the floor of the tunnel and having an adjustable width. The air flow for the jet was

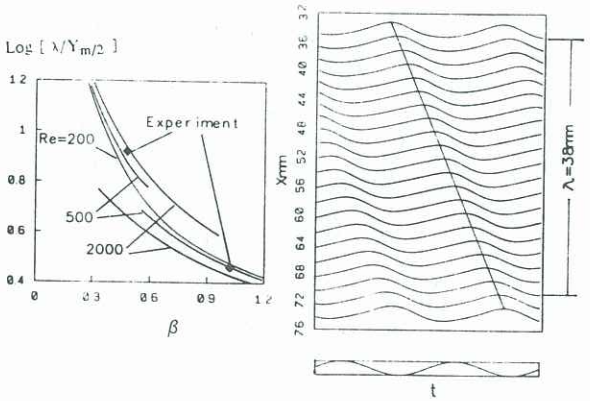

Fig.4 Wave length and phase velocity.

supplied by a centrifugal blower equipped with a speed controller which provided a very stable source of air. The jet emerged from the nozzle with a top-hat velocity profile. The two-dimensionality of the wall jet was checked and adjusted prior to the acquisition of data. The jet temperature was controlled within 0.1° C. The hot-wire data were acquired and analyzed digitally.

The placement of the wall jet in a closed-loop tunnel eliminated the adverse effects of room drafts which hinder the uniformity of the low speed laminar flow. The jet, however acts as an ejector and generates a slow uniform stream which did not exceed 5% of the jet velocity. The induced "free stream" velocity was subtracted from the data in the outer part of the wall-jet. The results for the natural flow are plotted on the left side of fig.1. The velocity profiles shifted to the right represent measurements at two forcing frequencies 14 & 29 hz. having an initial average longitudinal fluctuation level of 1%. At frequencies dominated by the "viscous" eigenmode the amplitude of forcing had to be curtailed to in order to reduce the distortion of the mean flow. Forcing the jet at the "inviscid mode" (at a frequency of 14 hz.) had no effect on its width while the rate of spread quintupled when the frequency of forcing at identical initial amplitude was increased to 66 hz. (fig. 1). The effect of excitation on the decay of the maximum jet velocity is much less spectacular, though in this case, the lowest frequency was the only one which retarded somewhat this rate of decay.

The downstream evolution of a constant frequency perturbation in the β - Re plane is shown in fig. 2 for the 3 frequencies mentioned above. By forcing the jet at 14 hz. one follows the amplification of the purely "inviscid mode" starting at the lower neutral stability curve. By forcing at 56 hz. one starts from the stable region located in the midst of the amplified zone and follows the amplification of the "viscous mode". The intermediate frequency starts in a region where the inviscid mode is amplified, then crosses into the region where both modes are amplified before entering the zone dominated by the pure "viscous mode".

The actual wave length of a traveling disturbance generated at a prescribed frequency was easily determined by moving the hot-wire probe in the streamwise direction and recording the velocity signal (fig. 4) which was phase-locked to the imposed oscillations. The wire was moved parallel to the surface starting at $Y = Y_{m/2}$ because the measured amplitude at that location is high and the phase does not abruptly change across the flow when $Y < Y_{m/2}$. The experimentally measured wave length and phase velocity agree very well with the predictions in spite of the fact that the divergence of the flow was not formally accounted for in the model (fig. 4). One may conclude that the phase velocity in a laminar wall-jet does not change appreciably over a single wave-length.

The amplitude and the phase distribution across the flow for the three frequencies of forcing is plotted in fig.5. Both distributions agree very well with the parallel flow model provided the disturbance is amplified over some fraction of its wave length. Consider the inviscid mode being excited by a constant frequency perturbation of 14 hz. As the perturbation crosses the neutral stability curve it carries with it all the spurious characteristics of the imposed signal (note the amplitude distribution measured

at X/b = 15, where b is the slot width) but soon after the predicted inviscid mode dominates the perturbation (fig.5a) with its characteristic maximum amplitude which is located in the vicinity of $Y = Y_{m/2}$. Forcing the jet at 56 hz. which initiates the perturbation in the stable "window" located at Re ≅ 400 (fig.2) behaves in a similar manner (fig 5b) for the viscous mode, but exciting the jet at 29 hz. yields initially a distribution of amplitudes appropriate to the "inviscid mode" which slowly shifts to the viscous one because the "inviscid mode" decays. The prediction for the decaying mode deteriorates with increasing X as the viscous mode starts to assert itself (figure 5c). In order to improve the prediction of the local amplitude of a perturbation in a laminar wall jet one has to account for the streamwise evolution of the disturbance itself and not only for the divergence of the mean flow.

files representing the flow over a concave surface are similar to fig.3 except that second instability eigenmode appears at a higher Re, while $Re_{crit.}$ remains unaffected. The introduction of convex curvature affects the neutral stability diagram more profoundly, though it too has little effect on $Re_{crit.}$ of either mode. The range of frequencies to which the flow is unstable is increased for both modes and the shape of the eigenfunctions is significantly altered. It appears that the identification of one mode with viscosity and the other with inviscid instability is an oversimplification because both are affected by the boundary conditions at the surface. Furthermore, as long as we do not know how to separate these modes in a clear way and how to prevent the non linear interaction between them we will have difficulties in modeling coherent structures in wall bounded flows.

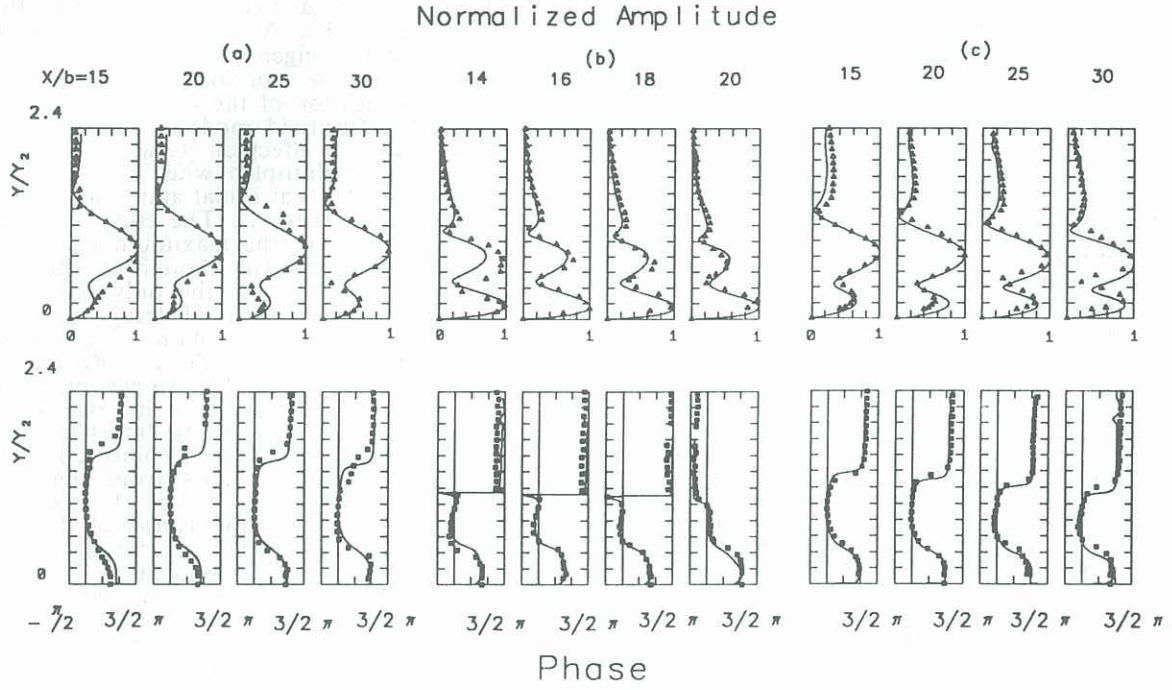

Fig.5 Amplitude and phase distributions, a comparison of experiment with theory.

CONCLUSIONS

The laminar wall jet is susceptible to two linearly amplifying modes of instability provided Re > 377. The phase velocity of each mode is different even when the dimensionless frequency β and the Re are identical. The same holds true for the form of the eigen functions. Thus the phase and amplitude distribution of the fluctuations across the flow depends on the particular mode considered. Only by a careful selection of parameters in an experiment one may follow the evolution of a pure mode over a limited spatial distance. In general both modes coexist and they can not be easily uncoupled.

One may solve the O-S equation for a variety basic state velocities U(y), of which Glauert's solution is a particular case. Such profiles represent wall jets flowing over logarithmic spirals which might be either concave or convex. The curvature of the surface affects the form of U(y) and in particular its slope near the wall which for a concave case is greatly increased. The neutral stability diagrams for pro-

REFERENCES

D.H., Chun and W.H., Schwarz, 1967, Phys. Fluids, 10, p.911

Cohen, J., Amitay, M. and Bayly, B.J., 1992, Phys. Fluids A 4, p.283

Glauert, M.B., 1956, J. Fluid Mech., 1, p.625

Liu, J.T.C., 1971, Phys. Fluids, 14,, p.2251.

Marasli, B. Champagne, F.H. and Wygnanski, I.J., 1989, J. Fluid Mech., 198, p.255

P., Mele, M., Morganti, M.F., Scibilia and A., Lasek, 1986, AIAA J., 24, p.938

Tam, C.K.W. and Chen, K.C., 1979, J. Fluid Mech., 92, p.303

Tsuji, Y., Morikawa, Y., Nagatani, T. and Sakou, M., 1977, Aeronautical Quarterly, Vol XXVIII, p.235

Weisbrot, I. and Wygnanski, I., 1988, J. Fluid Mech., 195, p.137-159

Katz, Y., Horev, E., and Wygnanski, I. 1992, J. Fluids Mech., 242, p.577